

On the lower energy limit of electronic stopping in simulated collision cascades in Ni, Pd and Pt

A. E. Sand^{a,*}, K. Nordlund^a

^a*Department of Physics, P.O. Box 43, FI-00014 University of Helsinki, Finland*

Abstract

We have investigated the effect of the choice of kinetic energy threshold T_c for electronic stopping (S_e) in molecular dynamics (MD) simulations of collision cascades. We find that while the choice of T_c has only a negligible effect in low energy cascades, it has a pronounced effect on the fraction of defects found in clusters in high energy cascades. In order to gain insight into the level of energy losses expected in cascades, we have simulated a large number of cascades in Ni, Pd and Pt, with primary knock-on atom (PKA) energies between 30 eV and 200 keV. Since the energy losses affect the total atomic displacements especially in high energy cascades, we use this measure to determine a reasonable value of T_c . By directly comparing the simulated mixing efficiency to ion beam mixing experiments, we conclude that a threshold of $T_c = 1$ eV is too low for simulations of high energy cascades in all materials considered. A value of $T_c = 10$ eV is more realistic, although for Pd and Pt, this results in a slight over-prediction of the mixing efficiency.

Keywords:

electronic stopping, collision cascades, molecular dynamics

1. Introduction

While primary radiation damage in metals has been studied by molecular dynamics (MD) simulations for decades [1], growing modern computer capacity enables increasingly large systems and higher energies to be modelled with this method [2]. Nevertheless, many aspects of the damage process remain under question. One of those is the treatment of inelastic energy losses and electron-phonon coupling during the collision cascade, and the effect of these on the final damage [3].

As we aim to understand the fundamental processes involved in radiation damage production, two main factors stand out. The importance for the fusion

*Corresponding author

Email address: `andrea.meinander@helsinki.fi` (A. E. Sand)

community of understanding neutron damage means that very high primary knock-on atom (PKA) energies must be considered, ranging up to hundreds of keV [4], while in contrast the main body of established simulation results mostly extends up to only tens of keV. The other aspect is the time frame of experiments, which far exceeds that accessible by MD. Direct experimental validation of cascade simulations is therefore difficult, and comparison to radiation damage often requires a multi-scale approach [5], where MD simulations provide input for kinetic Monte Carlo and rate theory models aimed at predicting radiation damage evolution. Since the morphology of the primary radiation damage is an important factor in determining the subsequent thermal evolution of defects [6, 7, 8], correct predictions of the structure of cascade debris is crucial for understanding the full process of radiation damage.

Collision cascades involve secondary recoils with a wide range of kinetic energies, in highly nonequilibrium situations from the initial ballistic phase through the thermalization and finally recrystallization of the heat spike [9]. The main effect of the coupling between electronic and ionic subsystems during the ballistic phase of the cascade is the electronic stopping S_e of energetic recoils, which is fairly well understood and motivated both experimentally and theoretically for higher energies (see e.g. [10] and references therein). In contrast, the energy transfer between the ionic and electronic subsystems in the liquid-like heat spike of a cascade is the result of a complicated interplay of effects, involving not only the coupling strength between the two systems, but also properties such as the electron heat capacity, mean free path and thermal conductivity [11, 12]. These material properties depend on temperature in a nontrivial way, influenced by the form of the density of states (DOS) of a given metal [13]. To further complicate the picture, the core of the heat spike is under-dense [9, 14, 15], and the validity of many theoretical models in this kind of material is uncertain. The question of the detailed response of the electronic subsystem in an energetic heat spike is therefore still unclear.

The electronic stopping power can be calculated, e.g., with SRIM [10]. It is readily incorporated into MD simulations as a frictional force on moving atoms, but requires the use of a kinetic energy cut-off T_c , below which the friction is not applied, else all thermal modes are quenched. Furthermore, although the SRIM stopping power is extrapolated down to zero kinetic energy, recent experiments and quantum mechanical simulations indicate that electronic stopping may not be linear wrt. velocity at lower energies (see e.g. [16, 17, 18]). In addition, this picture of energy losses is not valid at thermal energies, when the ionic and electronic subsystems are in equilibrium. However, the precise choice of T_c in simulations is somewhat arbitrary, and values vary in the literature [19, 20, 21, 22].

Although the correct treatment of energy transfer at lower energies is uncertain, momentum transfer in electron-ion collisions is negligible due to the large mass difference, so ionic trajectories are hardly perturbed. Therefore, the coupling between the two subsystems during the thermal phase mainly affects the rate of cooling of the heat spike. This, in turn, strongly influences the amount of atomic mixing which takes place as a result of the cascade, since

mixing during the thermal spike is an important part of the total atomic mixing [23]. Although the physics involved in the electronic stopping does not account for the full energy exchange during the thermal phase, the choice of S_e cut-off directly affects the rate of cooling of the heat spike. Because of this, a suitable choice of cut-off may be used as a first approximation to compensate for the lack of a direct treatment of electronic energy losses in the thermal phase of collision cascades.

In order to seek an optimal S_e cut-off, in this article we perform MD simulations of full collision cascades over a wide range of energies in Ni, Pd and Pt, and compare the simulated mixing efficiency with ion beam mixing (IBM) experiments. These elements were chosen because of the availability of reliable IBM measurements at low temperatures using marker layers. Since the main contribution to atomic mixing in metals stems from atom motion in the liquid-like heat spike [23, 14], chemical effects may enhance the mixing efficiency. We therefore compare to IBM experiments where the effect of diffusion of the tracer impurity is minimized by using tracer impurities that are chemically and physically as similar as possible to the matrix element. The total atom displacement in MD simulations can then be directly compared to the mixing efficiency in such experiments [24]. From this material selection we can also see the effect of atomic mass, which affects subcascade break-up and thus also the size of heat spikes, and through this the rate of cooling and the impact in simulations of the S_e low-energy threshold. Since the duration of the heat spike affects the degree of mixing which takes place in the cascade, a realistic rate of cooling in the simulation can be expected to result in a mixing efficiency comparable to the experimental measurements. The low temperatures (6 and/or 77 K) at which the experiments were performed excludes the possibility of prolonged duration of the heat spike due to the ambient temperature.

A detailed analysis of 150 keV cascades in W [25, 26] has shown that the choice of T_c has a strong effect on defect clustering when varied between 1 and 10 eV. **This is due to the presence of recoils with kinetic energies above 10 eV lasting only during the ballistic phase of the cascades. Thus, with $T_c = 10$ eV, electronic energy losses cease after this point, while with $T_c = 1$ eV, the electronic stopping continues into the thermal phase.** On the other hand, only a marginal effect is seen when T_c varies between 10 and 100 eV, **when in all cases the electronic energy losses cease roughly at the end of the ballistic phase. The fractal energy landscape of the ballistic phase [25] is expected to be largely independent of lattice structure.** We therefore compare simulations with $T_c = 1$ eV and $T_c = 10$ eV also in this work.

2. Methods and analysis

2.1. Cascade simulations

Full collision cascades in Pt, Pd and Ni were simulated using the classical molecular dynamics code PARCAS [27]. Cascades were performed with PKA energies ranging from 30 eV up to 200 keV, chosen in random directions. **We**

have performed a total of 30 simulations at each energy below 1 keV, 10 simulations for each energy between 1 and 20 keV, and 5 cascades for each energy above 50 keV. Periodic boundaries were used, with a Berendsen thermostat [28] applied to the border atoms to remove excess heat and quench pressure waves emanating from the cascade core. All simulations were performed at an ambient temperature of 0 K. The cell borders were monitored, and no energetic atoms with kinetic energy above 10 eV were allowed to pass the periodic boundary, else the simulation was aborted and restarted with the recoil further away from the boundary. In this way it was insured that all cascades remained within the cell, and did not self-interact. For the highest energy cascades, this required the use of systems of over 13 million atoms.

Embedded atom method (EAM) potentials were used for all three elements. The potentials for Pt and Pd were modified at distances closer than the nearest neighbor separation, in order to reproduce the experimental melting points of the materials [24]. This is necessary since the melting point strongly affects the duration of the liquid area, and thus also the atomic mixing which takes place during the cascade [29, 22]. All potentials were smoothly joined to the universal ZBL repulsive potential [30] at short distances.

No model of electron-phonon coupling [12] was used, but inelastic energy losses were included through electronic stopping, which was incorporated as a friction term, and applied to all atoms with kinetic energies above a certain threshold T_c . The magnitude of the stopping power is given by SRIM [10], and threshold values of both $T_c = 1$ eV and $T_c = 10$ eV were used for each material at all energies.

Defects were detected using an automated Wigner-Seitz cell method [31]. Clusters were also identified with an automated procedure, where a defect is defined as belonging to a cluster if it lies within a given cut-off radius to another defect. In the higher energy cascades many clusters included both vacancies and interstitials, and in this case the net defect numbers are reported.

In order to identify defects belonging to mixed clusters, the same cut-off needs to be used for both interstitials and vacancies. Although interstitial pairs are binding at larger distances than first nearest neighbors (1NN), the clustered fraction of SIAs was not affected by a cut-off including 1NN or 3NN (third nearest neighbors). This is due to the fact that the SIA clusters that form in a cascade are dense, and single SIAs lie well separated from others. The situation is different for vacancies, which are gathered in the center of a cascade, but typically fairly sparsely distributed. The clustered fraction of vacancies is therefore strongly affected by the choice of cut-off radius. Since the 1NN divacancy is the most stable, and 2NN divacancies may be either binding or repulsive [32, 33], we have chosen to perform the analysis for all materials using the 1NN distance criterion.

2.2. Atomic mixing

The mixing efficiency is directly derived from the cascade simulations, using the same method as in Ref. [24]. Briefly, the incident Kr ions give rise to energetic recoils within the material, creating subcascades which at these energies

do not significantly overlap [34]. The recoil energy spectrum is calculated for each experimental ion energy and ion-substrate combination using molecular dynamics range calculations [35]. The square of the total atom displacements R_{sim}^2 in isolated subcascades of different energies is obtained from the MD simulations detailed above. We then integrate R_{sim}^2 over the whole energy range of possible recoils, weighted by the primary recoil spectrum $n(E)$ of the Kr beam. We have fitted the total atom displacement R_{sim}^2 from the simulations to the function

$$R^2(E) = a \frac{E^{c+1}}{b^c + E^c} \quad (1)$$

in order to enable interpolation between the simulated data points. Here, a , b and c are fitting parameters. The simulated mixing efficiency is then given by

$$Q_{sim} = \frac{\int_0^{E_0} R^2(E)n(E)dE}{6n_0E_{D_n}} \quad (2)$$

where E_0 is the initial implantation energy, n_0 the atomic density and E_{D_n} the nuclear damage energy of the Kr beam as determined from the MD range calculations.

3. Results

3.1. Morphology of primary damage

The number of surviving defects is unaffected by the choice of T_c in cascades up to 10 keV, for all materials considered in this study. For PKA energies above 20 keV, small differences appear, with more surviving defects in cascades with $T_c = 10$ eV. Overall, the variation of defect numbers increases with increasing energy, though the largest effect is seen for the heaviest element, Pt. Cascades with 200 keV PKAs in Pt exhibited huge variations in defect numbers with $T_c = 10$ eV, where net defect numbers ranged from 203 to as much as 1328, due to the occasional formation of very large clusters. The numbers of surviving defects for all materials are shown in Figure 1.

Defect clustering also becomes sensitive to the electronic energy losses in the energy range between 10 and 20 keV. The fraction of defects in clusters is shown in Figure 2. We show here the fraction of SIAs in clusters with more than three defects, since the effect of T_c is seen specifically in the frequency of occurrence of larger clusters. For vacancies, the overall clustering is less than for SIAs, and the effect of T_c is clear for all cluster sizes. We therefore show the fraction of vacancies in clusters of any size, since this value has better statistics. Nevertheless, for both types of clusters, the values at the lower end of the energy spectrum vary strongly. Due to the small overall number of defects in low energy cascades, the occurrence of a single cluster has a large impact on the clustered fraction.

Larger clusters are formed in simulations with $T_c = 10$ eV than with $T_c = 1$ eV in all materials. With a higher cut-off, the heat spike has a longer time

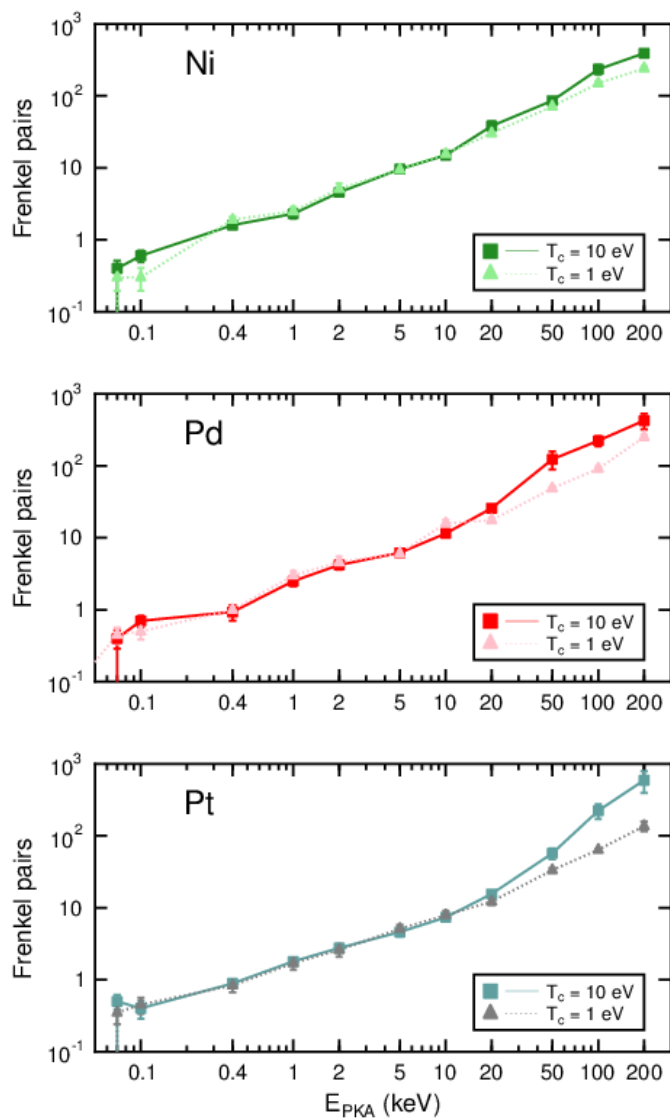


Figure 1: (Color online) Numbers of surviving defects from simulations with different T_c .

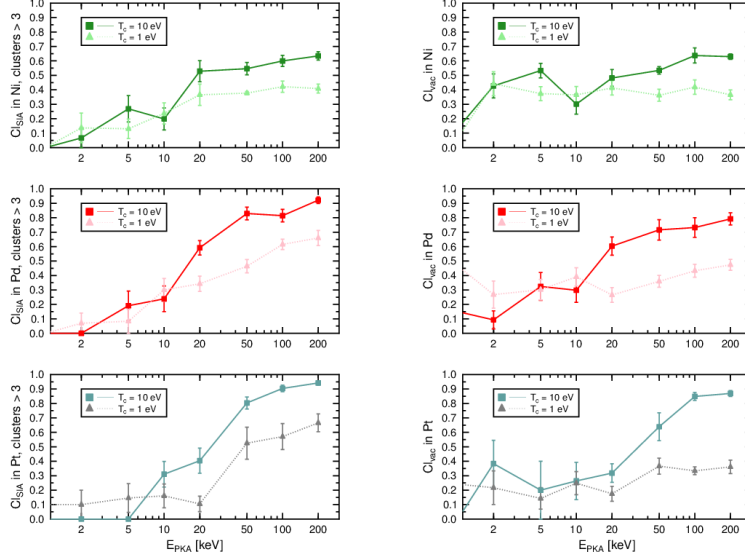


Figure 2: (Color online) The fraction of SIAs found in clusters larger than three, and the fraction of clustered vacancies (cluster size ≥ 2), from simulations with different T_c .

to thermalize before recrystallizing, providing more time for SIA clusters to nucleate in the high density region surrounding the liquid core. The slower recrystallization also allows vacancies to move towards the core before becoming frozen in the crystal [36], resulting in a larger fraction of both types of defects in clusters. A compact liquid region thus enhances the formation of larger clusters, since it takes longer to cool due to the smaller surface to volume ratio. The largest clusters will therefore begin to form at energies just below the point of subcascade break-up. The effect of the subcascade threshold between 20 and 50 keV in Ni is seen in the levelling out of the clustered fraction of interstitials. For the heavier Pt, on the other hand, many cascades are unbroken even at 200 keV, and correspondingly the clustered fraction exhibits a steady rise over the whole energy interval studied here.

Comparing the cumulative electronic energy losses in 200 keV cascades in Ni and Pt (Fig. 3), we see that the effect of a lower S_e cut-off is more pronounced in the heavier element Pt. Energy losses reach a maximum earlier in Ni than in Pt for both values of T_c , indicating that energetic recoils survive for longer in the denser heat spikes in Pt. The difference is especially clear when $T_c = 1$ eV, where the electronic energy losses accumulate in Pt for a full 10 ps.

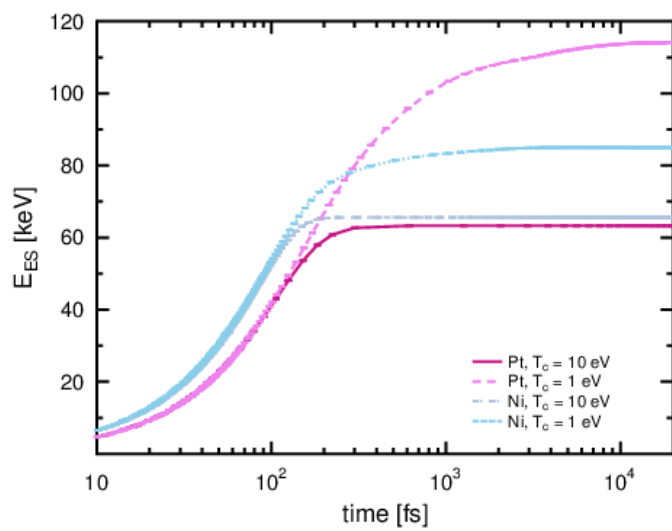


Figure 3: (Color online) The cumulative energy lost to electronic stopping in cascades with different T_e . Energy losses in Pd are qualitatively similar and lie between Ni and Pt; these are not included, in the interest of clarity.

3.2. Mixing efficiency

The recoil spectrum in all elements is dominated by low energy recoils (Fig. 4). Despite this, the main contribution to Q_{sim} comes from the high energy recoils, due to the fact that the total atomic displacement R^2 can increase by almost two orders of magnitude for one order of magnitude increase in the PKA energy (Fig. 5).

A good fit of the function in Eq. 1 to the lower energy simulation data was obtained with an exponent $c = 0.5$. However, because of the importance of the high-energy end of the spectrum, different exponents were tried in order to improve the fit to the high-energy cascades. In some cases good fits were obtained with different values of the exponent, ranging between 0.3 and 0.7. The variation of Q_{sim} predicted with the different curves is reflected in the uncertainty of the reported value. In particular, because of the large variation in 200 keV Pt cascades, the predicted total atomic displacement from five cascades has a relatively large uncertainty, and as a result also the fit to Eq. 1 and the calculated mixing efficiency has a large uncertainty.

Experimental and simulated mixing efficiencies are given in Table 1. The simulated mixing efficiency shows a large dependence on the T_c parameter. The effect in Ni is the smallest, probably due to the lower subcascade threshold for the lighter Ni, which restricts the size and thus the duration of the melt. For Ni, Q_{sim} agrees very well with experiment when $T_c = 10$ eV, while for Pd and Pt the higher threshold results in an overprediction of the efficiency. However, in simulations with $T_c = 1$ eV, Q_{sim} is clearly too low in all three materials. Figure 5 shows the impact of the choice of T_c on the calculation of Q_{sim} for 1 MeV Kr in Pt.

This indicates that although 1 eV was recommended as the cut-off value in Ref. [19] based on TDDFT calculations of a hypothetical one-electron metal, this calculation is not necessarily relevant to real metals. Furthermore, due to computational limitations, the study only extended up to PKA energies of 1 keV, and does not therefore give a description of the heat spike regime. **While excessive cooling of the heat spike resulting from a low value of T_c strongly inhibits clustering, only negligible effects are seen on the primary defect population for a wide range of higher T_c values [26]. Thus, despite the overprediction of Q in some cases, a value of $T_c \approx 10$ eV is recommended for the S_e cut-off in high energy cascades, to avoid too rapid quenching of the heat spike.**

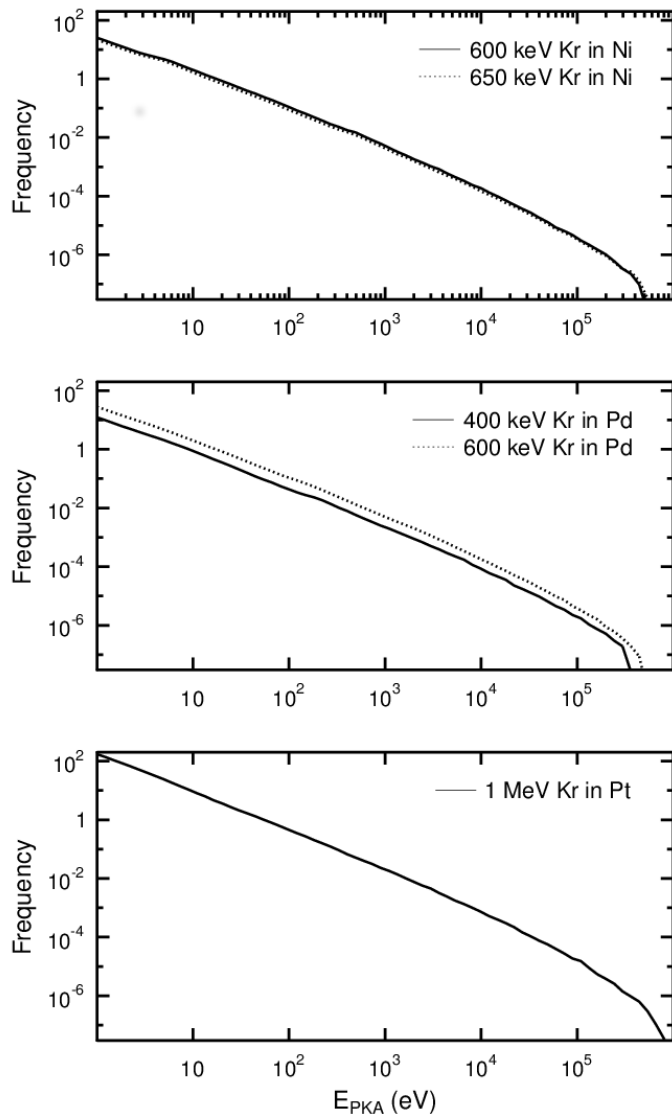


Figure 4: (Color online) The simulated recoil spectra for the experimental ion energies compared to in this work.

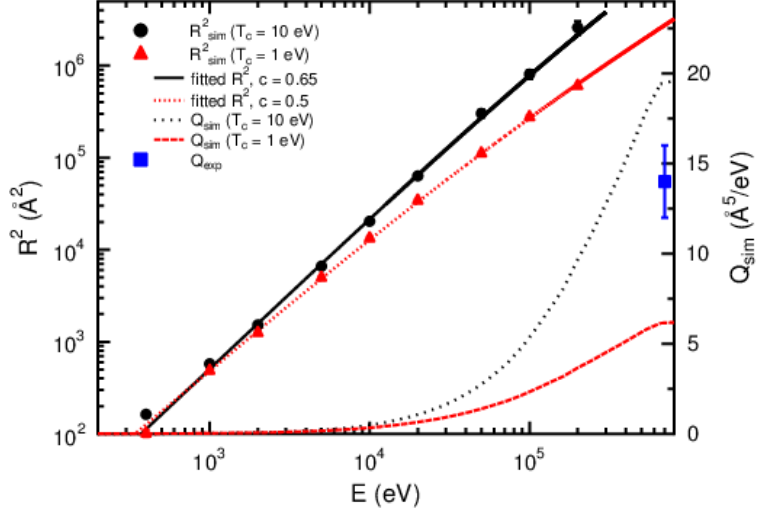


Figure 5: (Color online) The square of the total atom displacement from simulations in Pt with different T_c , and the function from Eq. 1 fitted to the data. The plot also shows the resulting integrated mixing efficiency for 1 MeV Kr in Pt.

Material	Beam	Q_{sim} ($\text{\AA}^5/\text{eV}$)	Q_{sim} ($\text{\AA}^5/\text{eV}$)	Q_{exp} ($\text{\AA}^5/\text{eV}$)
		$T_c = 1$ eV	$T_c = 10$ eV	
Ni	600 keV Kr	2.9 ± 0.1	4.7 ± 0.1	4.8 ± 0.5^a
Ni	650 keV Kr	3.1 ± 0.2	5.1 ± 0.1	5.0 ± 0.7^b
Pd	600 keV Kr	6.2 ± 0.2	14 ± 1	8.4 ± 0.8^a
Pd	400 keV Kr	6.1 ± 0.2	13.7 ± 0.5	9 ± 1^c
Pt	1 MeV Kr	6.1 ± 0.3	20 ± 3	14 ± 2^b

Table 1: Simulated and experimental values for the mixing efficiency Q . ^a Ref. [24] ^b Ref. [23] ^c Ref. [34]

4. Discussion and conclusions

Many cascade simulations reported in the literature have been performed without including S_e or other electronic effects. The results of these simulations are related to actual radiation damage through the concept of damage energy, which is the initial energy of the PKA minus the amount of energy lost in inelastic collisions with electrons. When S_e is not included, the initial PKA energy is effectively equal to the damage energy. In order to relate these simulations to experimental results, the actual recoil energy can be calculated [3], e.g. using an approximation to Lindhard's theory (LSS) which is the basis for the NRT standard [37] for estimating the level of experimental nuclear energy deposition. Alternatively, a convenient measure for simulated radiation damage is the efficiency with respect to the NRT prediction. The NRT formula, which itself is a function of the damage energy, gives the number of displaced atoms N_{NRT} as $N_{NRT} = 0.8E_{dam}/2E_d$, where E_{dam} is the damage energy and E_d is the material specific threshold displacement energy. Thus any comparison to experiment hinges critically on the amount of damage energy in a cascade.

However, there are several issues which make use of the damage energy in this way uncertain. Firstly, there is an inconsistency between the damage energy calculated by the LSS method, and the defect number production according to the NRT equation. As Robinson [38] points out, since atoms below $2 E_d$ do not contribute to the damage production, the electronic energy losses which stem from such atoms should not be subtracted from the total damage energy used in the NRT equation. Secondly, Lindhard's theory is based on an analysis of cross sections and energy transfer in energetic binary collisions, and is not valid at thermal energies. In addition, when energetic recoils become encompassed in the underdense and highly excited region of a thermal spike, this picture may cease to be valid already in the energy range considered here for T_c . Finally, in simulations where the electronic energy losses are taken into account, the damage energy is directly given from the simulation. However, it then depends crucially on the S_e cut-off, and can vary considerably for different T_c .

Figure 6 shows the damage energy from MD simulations in Pt, Pd and Ni with different T_c , and for comparison, the damage energy as calculated with the approximation to Lindhard's theory given in Ref. [37]. For Pt and Pd, the calculated damage energy agrees closely with that obtained using $T_c = 10$ eV, while for Ni the situation is more complicated, with good agreement at lower energies using $T_c = 10$ eV, while for the higher energies considered in this study, the calculated value approaches that obtained using $T_c = 1$ eV. The difference in damage energy obtained from simulations with different T_c is especially pronounced in Pt, due to its higher mass, and thus denser heat spike and more dominant liquid phase. In general, the heavier the element (and consequently the more massive the heat spikes), the better agreement is with LSS when $T_c = 10$ eV. For all elements, the amount of energy lost to the electrons when $T_c = 1$ eV exceeds that given by LSS.

In the absence of a direct treatment of electrons, we seek a solution to calculating energy losses which indirectly accounts for the possible heating of

the ionic system by the excited electronic system. Since the LSS calculation only considers energy transfer from ions to electrons, this should give an approximate upper bound to the total energy which is dissipated from the cascade area by the electronic system. Since heating of the ionic system by the electrons, if it occurs, can be expected to mainly affect the duration of the heat spike, we reach the same end result by restricting the amount of energy lost to electronic stopping. Furthermore, adjusting the value of T_c leaves the initial energy losses during the ballistic phase of the cascade untouched (Fig. 3), since at that point only high energy recoils exist. Only energy losses during the thermal phase of the cascade are thus affected, at precisely the time when the electronic system has acquired energy from the ballistic recoils and may transfer some of that energy back to the ions.

The defect production efficiency ξ for Pt and Ni is shown in Fig. 7. It is given by the ratio of the MD predicted number of Frenkel pairs N_{FP} over the NRT predicted defect numbers N_{NRT} , with E_{dam} determined from the simulations. Below 20 keV ξ turns out to be almost independent of T_c , despite the large difference in energy losses. Although ξ is only a small fraction due to the in-cascade recombination, this shows that the dependence of defect numbers on total available damage energy is rather robust. The efficiency is marginally higher at intermediate energies when $T_c = 1$ eV, since the single defects produced during the ballistic phase of the cascade have less time to recombine during the rapid cooling of the heat spike. On the other hand, for the highest energy cascades in Pt, when $T_c = 10$ eV and the heat spike is allowed to thermalize for a longer period, very large clusters are formed. The most massive, spherical 200 keV cascade produced four large interstitial clusters with up to 500 single SIAs, and a central vacancy cluster with 1300 single vacancies. The huge SIA clusters bind the defects, thus inhibiting their athermal recombination. This causes a marked rise in the efficiency not seen for the lighter elements Ni and Pd, nor when the rate of cooling of the heat spike is faster, with $T_c = 1$ eV. Since the level of defect clustering is of interest for predictions of long term radiation damage, a more detailed treatment of the energy transfer processes during the thermal phase of high energy cascades is needed.

In conclusion, we have studied the effect of electronic energy losses in simulated collision cascades in three fcc metals of varying atomic mass, Ni, Pd and Pt, using different values for the S_e cut-off T_c . Whereas the choice of T_c has little effect in simulations with PKA energies below 20 keV, the effect on the morphology of the surviving defects in higher energy cascades is substantial. Comparison of the simulated mixing efficiency to IBM experiments shows good agreement for Ni with $T_c = 10$ eV, while for Pd and Pt, Q is somewhat overestimated. However, for all three materials, Q is underestimated in simulations with $T_c = 1$ eV, clearly indicate that the quenching of the heat spike in the high energy cascades is too rapid. Thus a value of $T_c \approx 10$ eV is recommended. The total energy losses to electrons also exceeds the LSS prediction in high energy cascades when $T_c = 1$ eV.

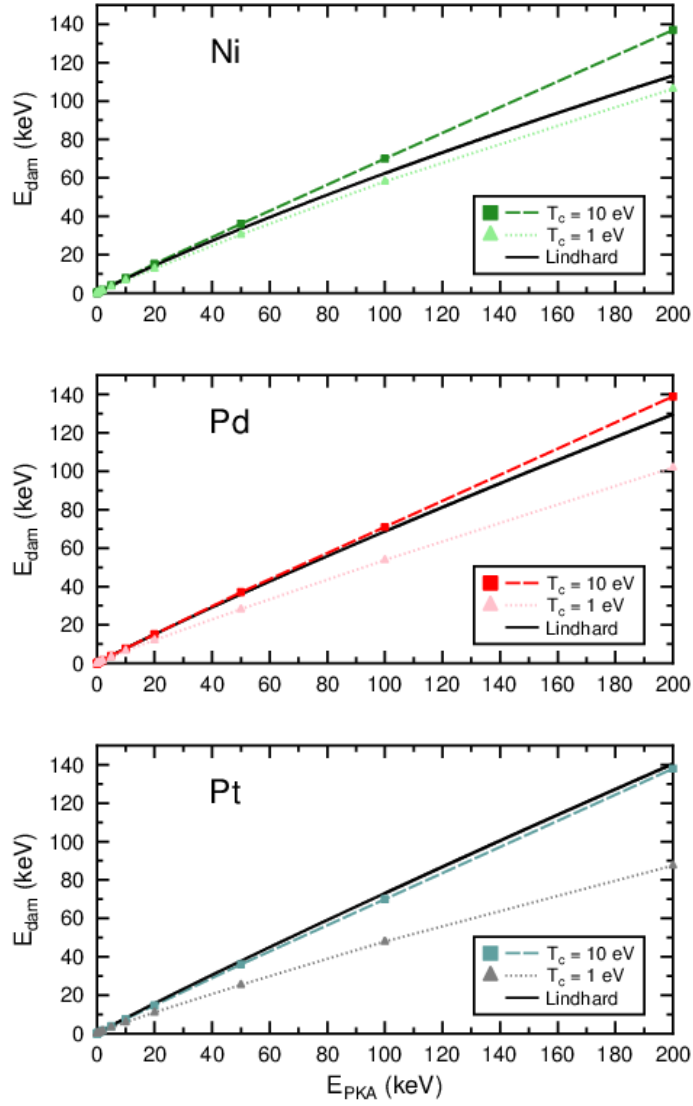


Figure 6: (Color online) The damage energy as derived from simulation, with different T_c , compared to the damage energy as calculated with the approximation to Lindhard's theory described in Ref. [37].

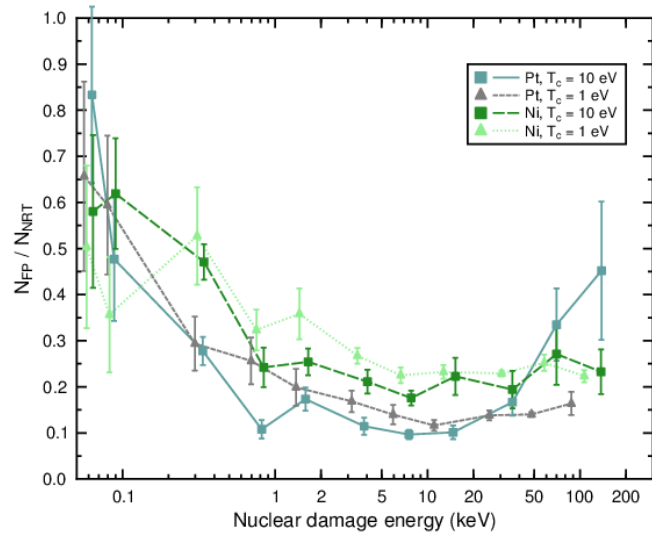


Figure 7: (Color online) The NRT efficiency for cascades in Pt and Ni, given by the ratio of the MD predicted number of Frenkel pairs N_{FP} over the NRT predicted defect numbers N_{NRT} , from simulations with different T_c . The efficiency for Pd lies in the same range as for Ni; it is not included, in the interest of clarity.

Acknowledgements

This project has received funding from Tekes – Finnish Funding Agency for Technology and Innovation – and the European Union’s Horizon 2020 research and innovation programme. The views and opinions expressed herein do not necessarily reflect those of the European Commission. AS also thanks Kulturfonden for a grant partially funding this work. Grants of computer time from the Centre for Scientific Computing in Espoo, Finland, are gratefully acknowledged.

- [1] J. B. Gibson, A. N. Goland, M. Milgram, G. H. Vineyard, *Phys. Rev.* 120 (1960) 1229–1253.
- [2] E. Zarkadoula, S. L. Daraszewicz, D. M. Duffy, M. A. Seaton, I. T. Todorov, K. Nordlund, M. T. Dove, K. Trachenko, *Journal of Physics: Condensed Matter* 25 (2013) 125402.
- [3] R. Stoller, in: R. J. Konings (Ed.), *Comprehensive Nuclear Materials*, Elsevier, Oxford, 2012, pp. 293 – 332.
- [4] M. Gilbert, S. Dudarev, S. Zheng, L. Packer, J.-C. Sublet, *Nuclear Fusion* 52 (2012) 083019.
- [5] C. Björkas, K. Nordlund, M. J. Caturla, *Phys. Rev. B* 85 (2012) 024105.
- [6] C. Becquart, C. Domain, L. Malerba, M. Hou, *Nuclear Instruments and Methods in Physics Research Section B: Beam Interactions with Materials and Atoms* 228 (2005) 181 – 186. Proceedings of the Seventh International Conference on Computer Simulation of Radiation Effects in Solids.
- [7] C. Becquart, A. Souidi, C. Domain, M. Hou, L. Malerba, R. Stoller, *Journal of Nuclear Materials* 351 (2006) 39 – 46. Proceedings of the Symposium on Microstructural Processes in Irradiated Materials.
- [8] D. Mason, X. Yi, M. Kirk, S. Dudarev, *ArXiv e-prints* (2014).
- [9] R. S. Averback, T. Diaz de la Rubia, in: H. Ehrenfest, F. Spaepen (Eds.), *Solid State Physics*, volume 51, Academic Press, New York, 1998, pp. 281–402.
- [10] J. F. Ziegler, SRIM-2008.04 software package, available online at <http://www.srim.org>, 2008.
- [11] I. Lifshits, M. Kaganov, L. Tanatarov, *Journal of Nuclear Energy. Part A. Reactor Science* 12 (1960) 69 – 78.
- [12] C. P. Flynn, R. S. Averback, *Phys. Rev. B* 38 (1988) 7118–7120.
- [13] Z. Lin, L. V. Zhigilei, V. Celli, *Phys. Rev. B* 77 (2008) 075133.
- [14] T. D. de la Rubia, R. S. Averback, R. Benedek, W. E. King, *Phys. Rev. Lett.* 59 (1987) 1930–1933.

- [15] M. Ridgway, T. Bierschenk, R. G. , B. Afra, M. D. Rodriguez, L. Araujo, A. P. Byrne, N. Kirby, O. H. Pakarinen, F. Djurabekova, K. Nordlund, M. Schleberger, O. Osmani, N. Medvedev, B. Rethfeld, W. Wesch, P. Kluth, *Phys. Rev. Lett.* 110 (2013) 245502.
- [16] J. E. Valdés, C. Parra, J. Díaz-Valdés, C. D. Denton, C. Agurto, F. Ortega, N. R. Arista, P. Vargas, *Phys. Rev. A* 68 (2003) 064901.
- [17] S. N. Markin, D. Primetzhofer, P. Bauer, *Phys. Rev. Lett.* 103 (2009) 113201.
- [18] J. M. Pruneda, D. Sánchez-Portal, A. Arnau, J. I. Juaristi, E. Artacho, *Phys. Rev. Lett.* 99 (2007) 235501.
- [19] J. le Page, D. R. Mason, C. P. Race, W. M. C. Foulkes, *New Journal of Physics* 11 (2009) 013004.
- [20] C. Björkas, K. Nordlund, *Nuclear Instruments and Methods in Physics Research Section B: Beam Interactions with Materials and Atoms* 267 (2009) 1830 – 1836.
- [21] D. M. Duffy, A. M. Rutherford, *Journal of Physics: Condensed Matter* 19 (2007) 016207.
- [22] K. Nordlund, M. Ghaly, R. S. Averback, M. Caturla, T. Diaz de la Rubia, J. Tarus, *Phys. Rev. B* 57 (1998) 7556–7570.
- [23] S.-J. Kim, M.-A. Nicolet, R. S. Averback, D. Peak, *Phys. Rev. B* 37 (1988) 38–49.
- [24] K. Nordlund, L. Wei, Y. Zhong, R. S. Averback, *Phys. Rev. B* 57 (1998) R13965–R13968.
- [25] A. E. Sand, S. L. Dudarev, K. Nordlund, *EPL* 103 (2013) 46003.
- [26] A.E. Sand, K. Nordlund, S.L. Dudarev, *Journal of Nuclear Materials* 455 (2014) 207 – 211.
- [27] K. Nordlund, *PARCAS* computer code. The main principles of the molecular dynamics algorithms are presented in [39, 40]. The adaptive time step is the same as in [35], 2006.
- [28] H. Berendsen, J. Postma, W. van Gunsteren, A. DiNola, J. Haak, *The Journal of Chemical Physics* 81 (1984) 3684–3690.
- [29] K. Nordlund, M. Ghaly, R. S. Averback, *J. Appl. Phys.* 83 (1998) 1238–1246.
- [30] J. F. Ziegler, U. Littmark, J. P. Biersack, *The stopping and range of ions in solids* / J.F. Ziegler, J.P. Biersack, U. Littmark, Pergamon New York, 1985.

- [31] K. Nordlund, R. S. Averback, *Phys. Rev. B* 56 (1997) 2421–2431.
- [32] E. H. Megchiche, C. Mijoule, M. Amarouche, *Journal of Physics: Condensed Matter* 22 (2010) 485502.
- [33] J.-M. Zhang, Y.-N. Wen, K.-W. Xu, V. Ji, *Journal of Physics and Chemistry of Solids* 69 (2008) 1957 – 1962.
- [34] I. Fenn-Tye, A. Marwick, *Nuclear Instruments and Methods in Physics Research Section B: Beam Interactions with Materials and Atoms* 18 (1986) 236 – 242.
- [35] K. Nordlund, *Computational Materials Science* 3 (1995) 448 – 456.
- [36] K. Nordlund, R. S. Averback, *Phys. Rev. B* 59 (1999) 20–23.
- [37] M. J. Norgett, M. T. Robinson, I. M. Torrens, *Nucl. Eng. Des.* 33 (1975) 50–54.
- [38] M. T. Robinson, O. S. Oen, *Jour. Nucl. Mater.* 110 (1982) 147–149.
- [39] K. Nordlund, M. Ghaly, R. S. Averback, M. Caturla, T. Diaz de la Rubia, J. Tarus, *Phys. Rev. B* 57 (1998) 7556–7570.
- [40] M. Ghaly, K. Nordlund, R. S. Averback, *Philosophical Magazine A* 79 (1999) 795–820.